Electronic Supplementary Material (ESI) for RSC Chemical Biology.

Supplementary Materials

Harnessing PD-L1 interface peptide for positron emission tomography imaging of PD-1 immune checkpoint

Kuan Hu et al.

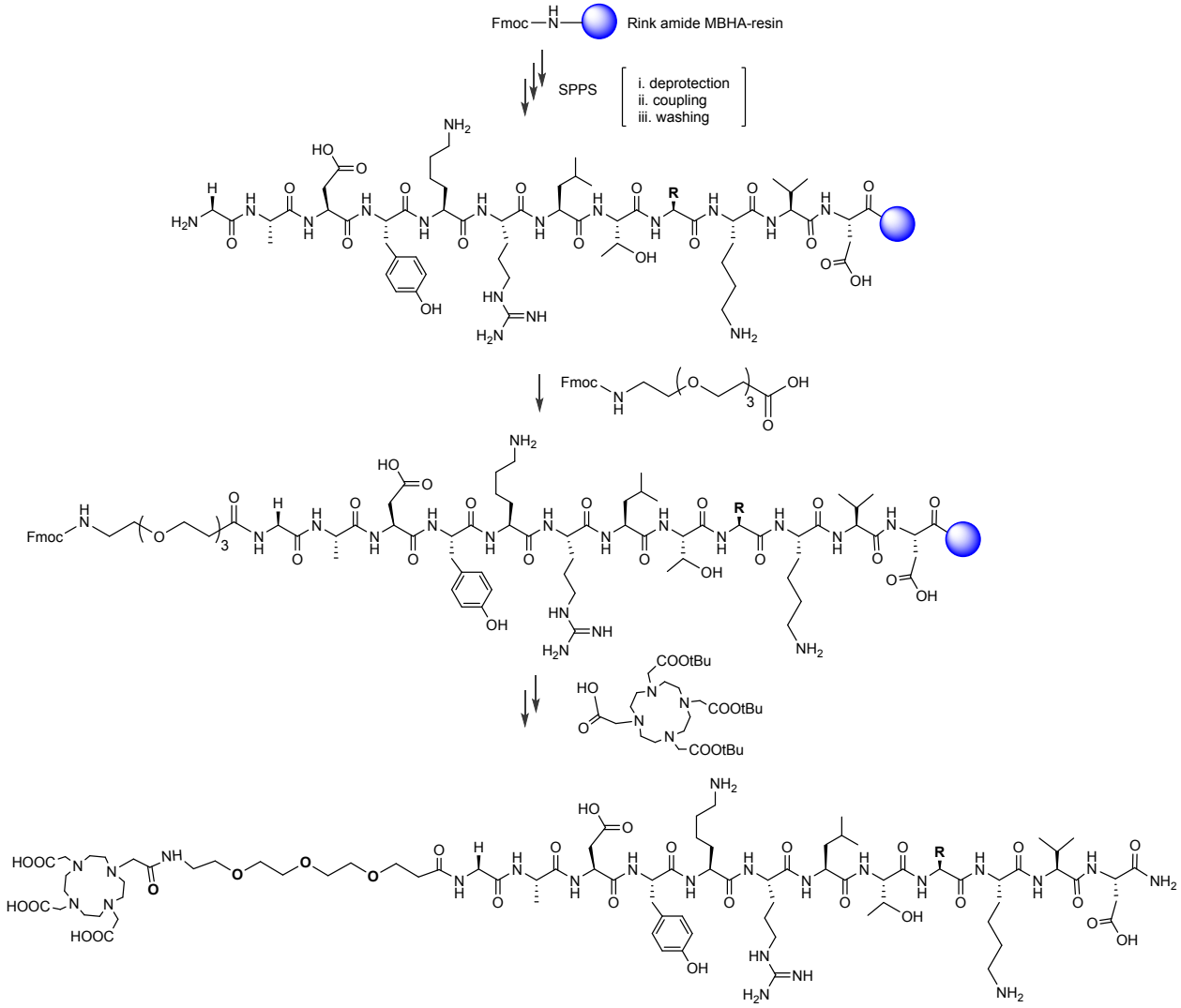

Scheme S1. Fmoc-based solid-phase peptide synthesis of m(h)-Pep-1. R group is the side chain of leucine in mPep-1-DOTA or the side chain of Valine in hPep-1-DOTA.

Table S1. Biodistribution of hPep-1-[^{64}Cu] in B16F10 tumor bearing mice (*n* = 3) at 5 min, 20 min, 40 min, and 100 min postinjection.

	5 min	20 min	40 min	100 min
organs	mean (%ID/g) ± SD	mean (%ID/g) ± SD	mean (%ID/g) ± SD	mean (%ID/g) ± SD
Blood	8.770 ± 0.573	3.374 ± 0.270	1.529 ± 0.081	0.470 ± 0.054
Heart	2.525 ± 0.421	1.160 ± 0.136	0.795 ± 0.016	0.664 ± 0.042
Lung	4.250 ± 0.638	2.386 ± 0.286	2.213 ± 0.038	2.090 ± 0.014
Thymus	1.560 ± 0.269	1.164 ± 0.226	0.938 ± 0.047	0.609 ± 0.157
Liver	2.721 ± 0.203	3.760 ± 0.511	4.751 ± 0.087	4.429 ± 0.134
Pancreas	1.588 ± 0.056	0.799 ± 0.068	0.642 ± 0.094	0.534 ± 0.119
Spleen	1.423 ± 0.212	0.718 ± 0.020	0.680 ± 0.129	0.431 ± 0.047
Kidney	20.728 ± 2.764	12.473 ± 0.542	10.978 ± 0.227	8.957 ± 0.701
Stomach	1.605 ± 0.188	1.981 ± 0.146	2.125 ± 0.121	1.798 ± 0.059
Small intestine	2.098 ± 0.103	2.634 ± 0.396	2.742 ± 0.067	2.700 ± 0.049
Int. lymph node	2.388 ± 0.415	0.972 ± 0.434	0.910 ± 0.200	0.578 ± 0.104
Muscle	1.703 ± 0.476	1.082 ± 0.485	0.301 ± 0.013	0.197 ± 0.008
Bone	1.545 ± 0.083	0.899 ± 0.061	0.763 ± 0.086	0.508 ± 0.049
Testis	1.154 ± 0.398	0.599 ± 0.016	0.543 ± 0.082	0.505 ± 0.076
Tumor	3.367 ± 0.867	2.603 ± 0.225	1.794 ± 0.031	1.486 ± 0.058
Brain	0.296 ± 0.046	0.114 ± 0.022	0.105 ± 0.002	0.079 ± 0.005

Table S2. Biodistribution of mPep-1-[^{64}Cu] in B16F10 tumor bearing mice (*n* = 3) at 5 min, 20 min, 40 min, and 100 min postinjection.

	5 min	20 min	40 min	100 min
organs	mean (%ID/g) ± SD	mean (%ID/g) ± SD	mean (%ID/g) ± SD	mean (%ID/g) ± SD
Blood	6.835 ± 0.356	2.310 ± 1.006	1.061 ± 0.135	0.320 ± 0.081
Heart	2.127 ± 0.090	0.986 ± 0.489	0.529 ± 0.088	0.440 ± 0.170
Lung	3.255 ± 0.101	1.954 ± 0.963	1.580 ± 0.229	1.637 ± 0.637
Thymus	1.154 ± 0.278	0.802 ± 0.288	0.660 ± 0.171	0.496 ± 0.132
Liver	2.467 ± 0.140	3.262 ± 1.476	3.698 ± 0.954	3.819 ± 1.308
Pancreas	1.323 ± 0.122	0.730 ± 0.287	0.471 ± 0.074	0.430 ± 0.148
Spleen	5.243 ± 0.285	2.456 ± 1.080	1.927 ± 0.354	1.268 ± 0.428
Kidney	22.840 ± 1.389	14.002 ± 6.441	11.310 ± 1.953	10.248 ± 3.691
Stomach	1.802 ± 0.127	1.265 ± 0.592	1.063 ± 0.255	1.637 ± 0.482
Small intestine	1.455 ± 0.155	1.550 ± 0.683	1.730 ± 0.687	2.215 ± 0.495
Int. lymph node	3.260 ± 0.866	0.558 ± 0.249	0.479 ± 0.123	0.404 ± 0.127
Muscle	1.391 ± 0.404	0.939 ± 0.285	0.455 ± 0.047	0.423 ± 0.245
Bone	1.256 ± 0.126	0.824 ± 0.321	0.958 ± 0.359	0.577 ± 0.124
Testis	1.209 ± 0.383	1.089 ± 0.454	0.698 ± 0.059	0.533 ± 0.211
Tumor	5.522 ± 1.353	4.475 ± 1.560	4.079 ± 1.323	1.887 ± 0.229
Brain	0.212 ± 0.012	0.126 ± 0.053	0.126 ± 0.038	0.058 ± 0.009

Table S3. A summary of PD-1 targeting radiotracers in references[1-11]. [a]The best time point for PET imaging after intravenous injection. [b]The ratios were calculated according to either the quantification of PET images or ex vivo biodistribution data.

Entry	Probe name	Tracer type	Molecular wight	Labeling	Timing	Major clearance organs	Tumor to blood ratio	Tumor to muscle ratio	Targeting specificity	Tumor type	Publishing year	reference
1	DOTA-PD-1	mAb	-	^{64C}u	24 h	liver, kidney	0.8	11	mouse	B16F10	2015	[1]
2	NOTA-PD-1	mAb	-	^{64}Cu	24 h	kidney, liver	-	-	mouse	B16	2016	[2]
3	nivolumab	mAb	146 Kda	^{89}Zr	24 h	liver	-	-	non-human primates	-	2016	[3]
4	PD-1-Liposome-DOX	liposome-mAb	-	^{64}Cu	12 h	liver, kidney	-	~10	mouse	4T1	2017	[4]
5	Pembrolizumab	mAb	149 Kda	^{89}Zr	24 h	liver, kidney	-	-	mouse	-	2017	[5]
6	Pembrolizumab	mAb	149 Kda	^{89}Zr and ^{64}Cu	24 h	liver, kidney	1.5-2	25	mouse	A375	2017	[6]
7	nivolumab	mAb	146 KDa	^{89}Zr	24 h	liver, kidney	2-4	5-8	mouse	A549	2018	[7]
8	Pembrolizumab	mAb	149 Kda	^{64}Cu	24 h	liver, kidney	1.5-2	~10	mouse	293T	2018	[8]
9	nivolumab	mAb	146 KDa	^{89}Zr	162 h	liver	-	-	human	NSCLC	2018	[0]
10	JS001	mAb	149 KDa	^{99m}Tc	8 h	kidney, liver	-	-	mouse	BCG823	2019	[10]
11	JS001	mAb	149 KDa	^{124}I	24 h	liver, kidney	1.5	8	mouse	S180	2020	[11]
12	mPep-1	peptide	~2 Kda	^{64}Cu	0.5-1 h	kidney	~4	~9	mouse	B16F10	2020	this study

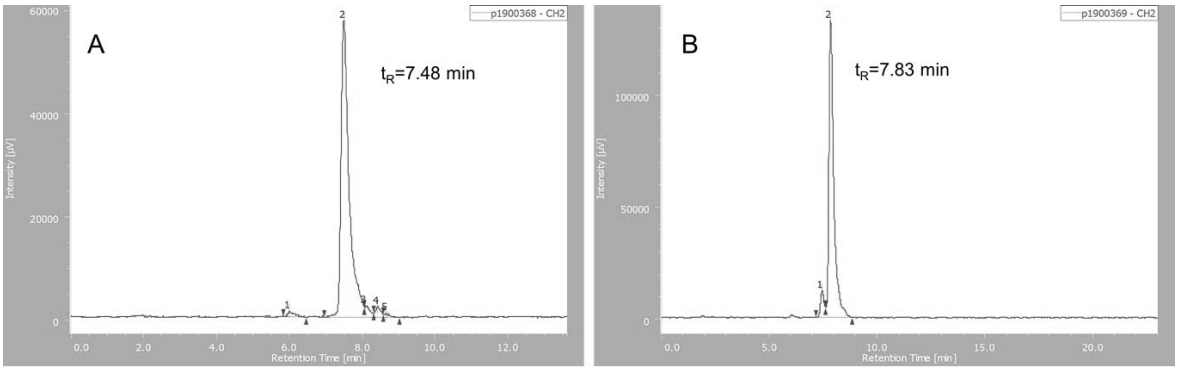

Figure S1. RP-HPLC chromatograms of hPep-1-[^{64}Cu] (A) and mPep-1-[^{64}Cu] (B).

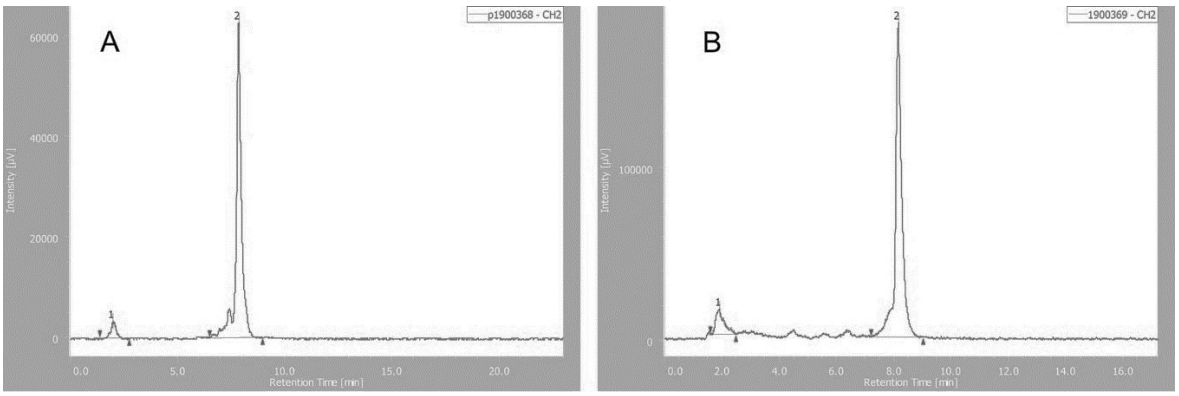

Figure S2. Stability analysis of hPep-1-[^{64}Cu] (A) and mPep-1-[^{64}Cu] (B) in mouse serum after 1 hour incubation.

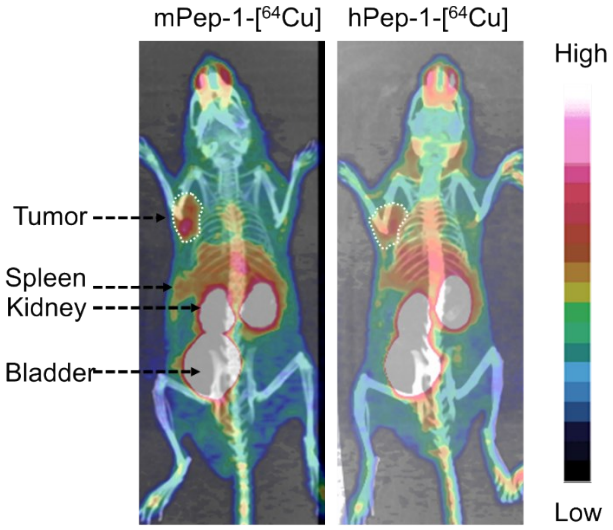

Figure S3. Representative maximum intensity projection (MIP) PET images co-registered with CT images in C57BL/6J mice bearing B16F10 show the whole-body of mouse after injected with mpep-1-[^{64}Cu] or hpep-1-[^{64}Cu] for 40 min.

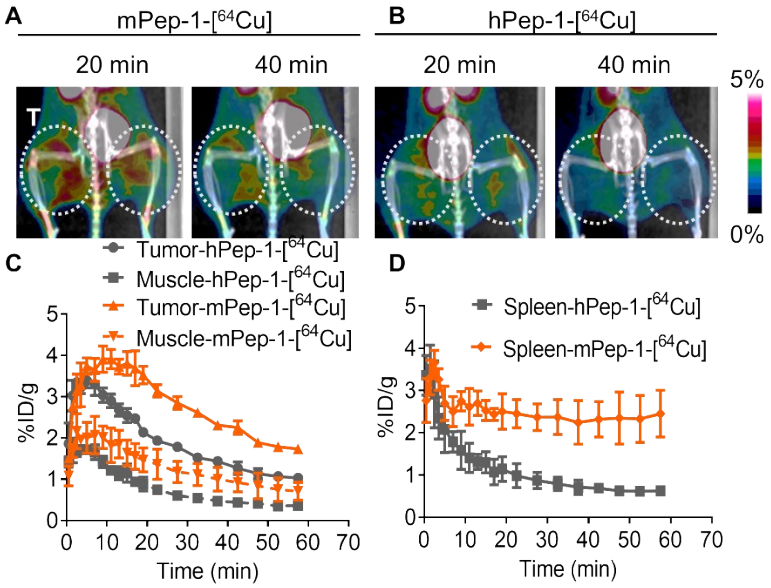

Figure S4. PET-CT co-registration images and regions of interest (ROI) curves of selected organs in C57BL/6J mice bearing-B16F10 tumors. MIPs PET-CT images of mice post-injection of (A) mPep-1-[^{64}Cu] and (B) hPep-1-[^{64}Cu] for 20 min and 40 min. The white dashed circles indicate the tumors. (C) Tumor and muscle (D) spleen uptakes were estimated from the ROI of PET-CT images.

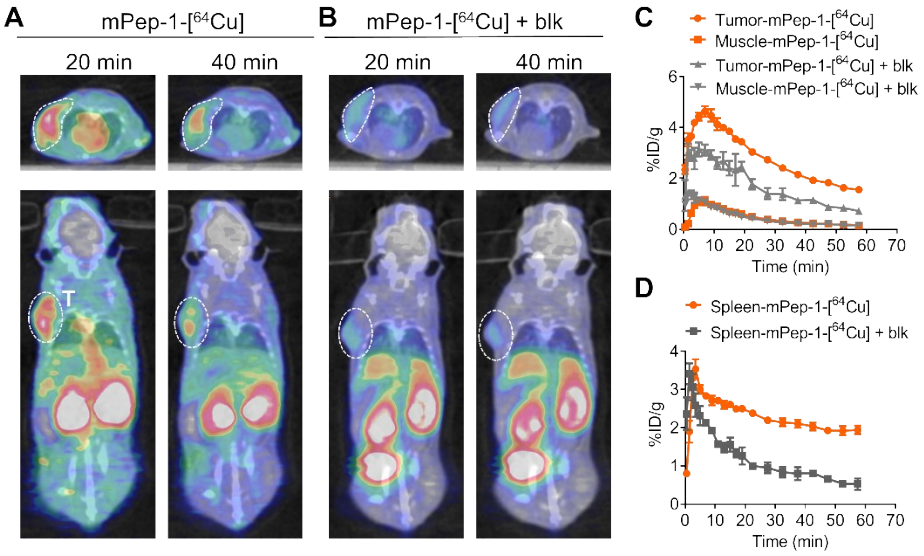

Figure S5. PET-CT co-registration images and regions of interest (ROI) curves of selected organs in B16F10-bearing C57BL/6J mice. Representative coronal and axial PET-CT images of mice post-injection of (A) mPep-1-[^{64}Cu] and (B) co-injection of mPep-1-[^{64}Cu] + mPep-1-DOTA (5 mg kg^{-1}) for 20 min and 40 min. Areas within the white dashed circles indicate the tumors. (C) Tumor and muscle and (D) spleen uptake was estimated from the ROI of PET-CT images, for each curve, the error bars represent standard deviations (SD), *n* =3.

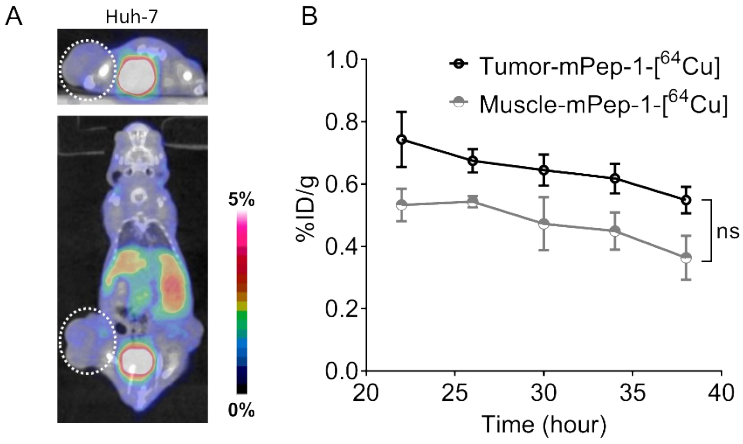

Figure S6. PET-CT images in Huh-7 bearing Balb/c nude mice. (A) Coronal and axial PET-CT images of mice post-injection of mPep-1-[^{64}Cu] for 20 min. The white dashed circles indicate the tumor. (B) Tumor and muscle uptakes were estimated from the ROI of PET-CT images.

Supplementary HPLC and Mass spectra

hpep-1-DOTA

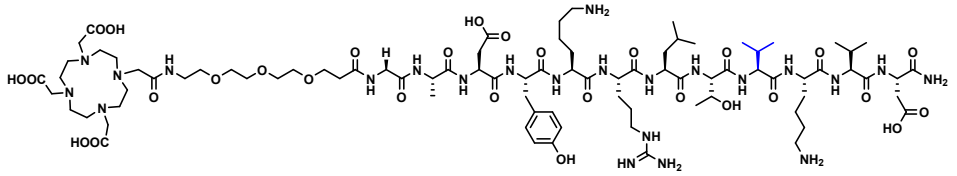

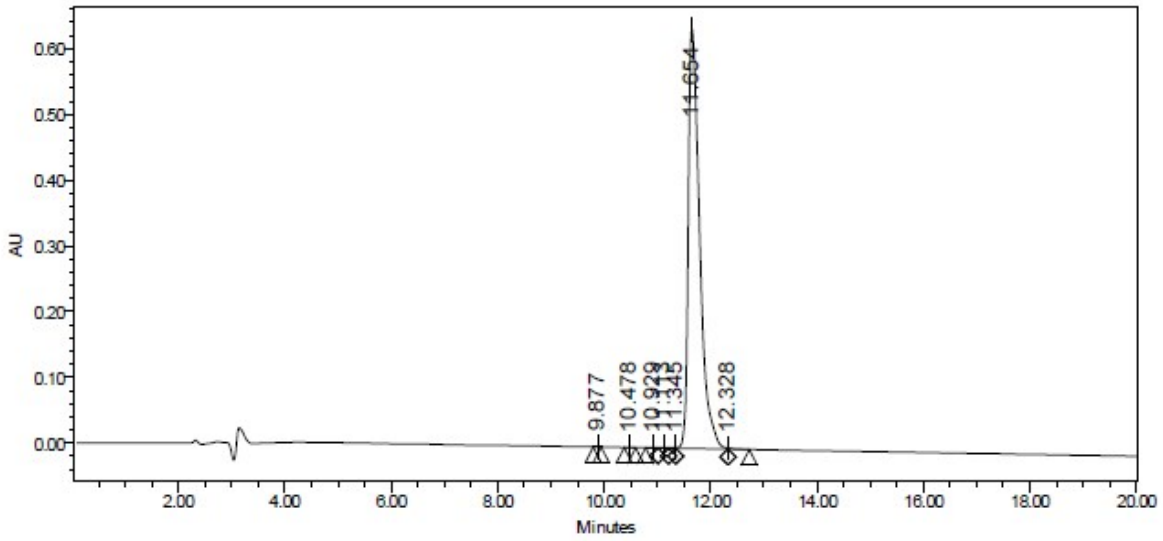

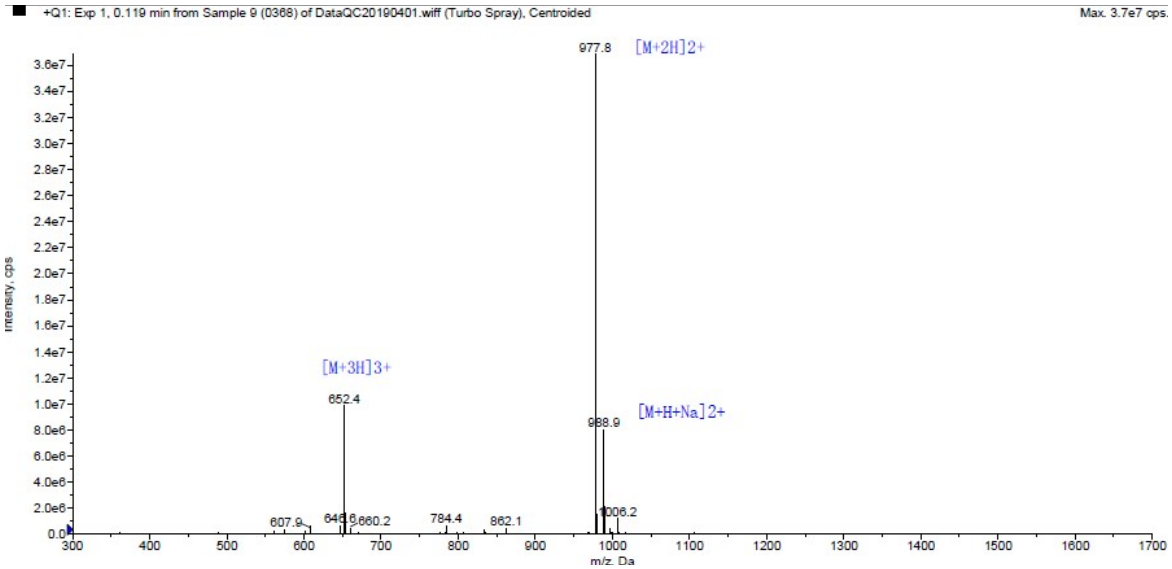

mpep-1-DOTA

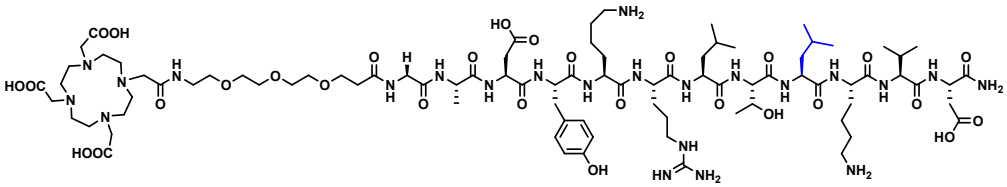

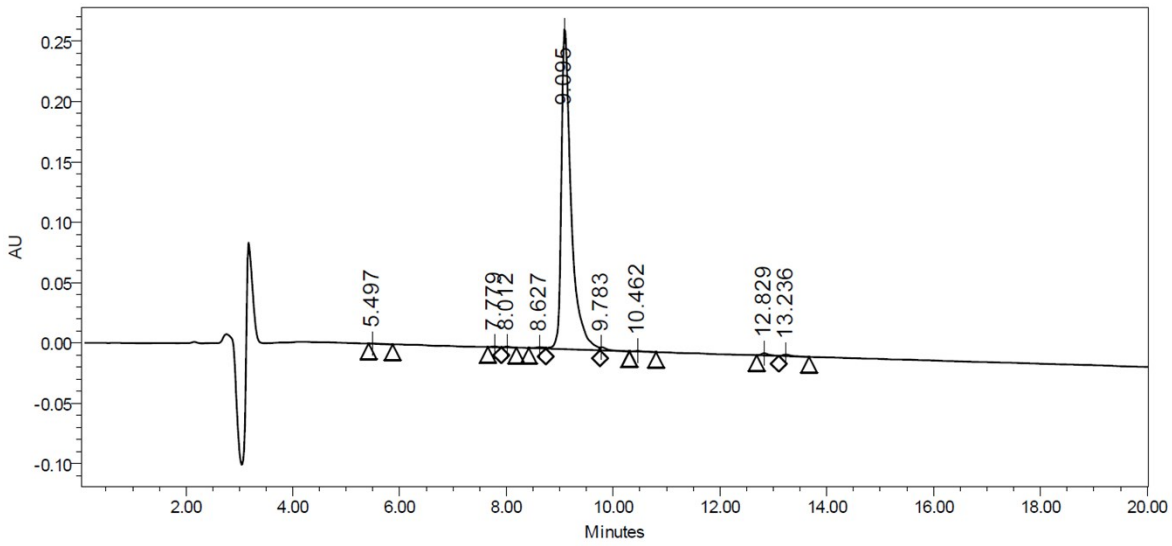
AU
Minutes
5.497
7.779
8.012
8.627
9.005
9.783
10.462
12.829
13.236

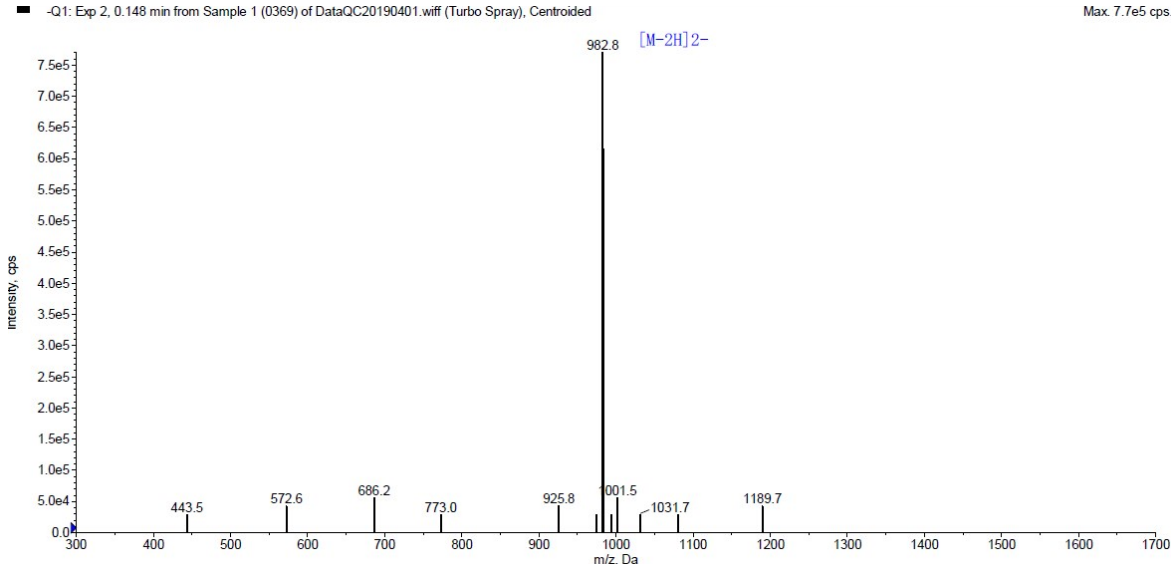
-Q1: Exp 2, 0.148 min from Sample 1 (0369) of DataQC20190401.wiff (Turbo Spray), Centroided
Max. 7.7e5 cps
[M-2H]2-
982.8
intensity, cps
m/z, Da
443.5
572.6
686.2
773.0
925.8
1001.5
1031.7
1189.7

1. A. Natarajan, A. T. Mayer, L. Xu, R. E. Reeves, J. Gano and S. S. Gambhir, *Novel Radiotracer for ImmunoPET Imaging of PD-1 Checkpoint Expression on Tumor Infiltrating Lymphocytes, Bioconjugate chemistry*, 2015, **26**, 2062-2069.
2. M. Hettich, F. Braun, M. D. Bartholoma, R. Schirmbeck and G. Niedermann, *High-Resolution PET Imaging with Therapeutic Antibody-based PD-1/PD-L1 Checkpoint Tracers, Theranostics*, 2016, **6**, 1629-1640.
3. E. L. Cole, J. Kim, D. J. Donnelly, R. A. Smith, D. Cohen, V. Lafont, P. E. Morin, R. Y. C. Huang, P. L. Chow, W. Hayes and S. Bonacorsi, *Radiosynthesis and preclinical PET evaluation of 89Zr-nivolumab (BMS-936558) in healthy non-human primates, Bioorganic & Medicinal Chemistry*, 2017, **25**, 5407-5414.
4. Y. Du, X. Liang, Y. Li, T. Sun, Z. Jin, H. Xue and J. Tian, *Nuclear and Fluorescent Labeled PD-1-Liposome-DOX-(64)Cu/IRDye800CW Allows Improved Breast Tumor Targeted Imaging and Therapy, Molecular pharmaceutics*, 2017, **14**, 3978-3986.
5. C. G. England, E. B. Ehlerding, R. Hernandez, B. T. Rekoske, S. A. Graves, H. Sun, G. Liu, D. G. McNeel, T. E. Barnhart and W. Cai, *Preclinical Pharmacokinetics and Biodistribution Studies of 89Zr-Labeled Pembrolizumab, Journal of Nuclear Medicine*, 2017, **58**, 162-168.
6. A. Natarajan, A. T. Mayer, R. E. Reeves, C. M. Nagamine and S. S. Gambhir, *Development of Novel ImmunoPET Tracers to Image Human PD-1 Checkpoint Expression on Tumor-Infiltrating Lymphocytes in a Humanized Mouse Model, Molecular imaging and biology : MIB : the official publication of the Academy of Molecular Imaging*, 2017, **19**, 903-914.
7. C. G. England, D. Jiang, E. B. Ehlerding, B. T. Rekoske, P. A. Ellison, R. Hernandez, T. E. Barnhart, D. G. McNeel, P. Huang and W. Cai, *(89)Zr-labeled nivolumab for imaging of T-cell infiltration in a humanized murine model of lung cancer, European journal of nuclear medicine and molecular imaging*, 2018, **45**, 110-120.
8. A. Natarajan, C. B. Patel, F. Habte and S. S. Gambhir, *Dosimetry Prediction for Clinical Translation of (64)Cu-Pembrolizumab ImmunoPET Targeting Human PD-1 Expression, Scientific reports*, 2018, **8**, 633.
9. A. N. Niemeijer, D. Leung, M. C. Huisman, I. Bahce, O. S. Hoekstra, G. A. M. S. van Dongen, R. Boellaard, S. Du, W. Hayes, R. Smith, A. D. Windhorst, N. H. Hendrikse, A. Poot, D. J. Vugts, E. Thunnissen, P. Morin, D. Lipovsek, D. J. Donnelly, S. J. Bonacorsi, L. M. Velasquez, T. D. de Gruijl, E. F. Smit and A. J. de Langen, *Whole body PD-1 and PD-L1 positron emission tomography in patients with non-small-cell lung cancer, Nature communications*, 2018, **9**, 4664.
10. X. Guo, H. Zhu, T. Liu, X. Xu, Y. Kong, S. Yao, X. Sheng and Z. Yang, *Development of (99m)Tc-conjugated JS001 antibody for in vivo mapping of PD-1 distribution in murine, Bioorganic & medicinal chemistry letters*, 2019, DOI: 10.1016/j.bmcl.2019.06.019.
11. H. Huang, H. Zhu, Q. Xie, X. Tian, X. Yang, F. Feng, Q. Jiang, X. Sheng and Z. Yang, *Evaluation of 124I-JS001 for hPD1 immuno-PET imaging using sarcoma cell homografts in humanized mice, Acta Pharmaceutica Sinica B*, 2020, DOI: 10.1016/j.apsb.2020.02.004.